Submitted to **Journal of the European Optical Society-Rapid Publications**
Template provided by EDP Sciences

Research article

The influence of temperature for the single-cycle biphotons generated by type-II SPDC in chirp QPM PPLN

Haibo Lin[1⋆,⋆⋆] and Jinbao Wang[1,⋆⋆]

[1] Institute of Mechanical & Electrical Technology, Taizhou Vocational & Technical College, Taizhou 318000, China

Abstract – We study the temperature-dependent type II spontaneous parametric down-conversion (SPDC) in the linearly chirped quasi-phase-matching (QPM) periodically poled lithium niobate (PPLN) crystal. The SPDC process can generate the biphotons with the single-cycle level. It shows that the chirp rate of the poled grating periods is the main influence factor for the phase matching function, frequency response range, Fedorov parameter and the count rate of the biphotons. Meanwhile, the temperature plays an important role for the type of $e \rightarrow o + e$, the higher temperature makes the frequency response range be wider, Fedorov parameter and count rate be higher. Meanwhile, the appropriate chirp rate and temperature can help the type II SPDC generate the single cycle biphotons in chirp QPM PPLN.

Keywords. Biphotons, SPDC, Single cycle, entanglement

1. Introduction

In recent decades, it has been aroused widespread interest in the generation of ultrashort pulse with single- or even sub-cycle level[1, 2, 3, 4, 5, 6]. It has deep development in THz, visible and extreme ultraviolet range[7, 8, 9], including the theoretical and experimental researches about the generation of ultrashort pulse[10, 11, 12]. Among these methods about the generation of ultrashort pulse, the way of generation for biphotons by the spontaneous parametric down conversion (SPDC) could reach the narrower temporal width within single level[13, 14, 15]. Meanwhile, the ultrashort biphotons could show some special characteristics such as entanglement, which is widely applied in quantum information[16, 17, 18, 19].

The biphotons, generated by SPDC, could show high entanglement degree and ultrashort temporal width with single cycle level. However, the conversion efficiency of pump photon converting to signal and idler photons is quite low. It means that it cannot effectively rise the count rate of biphotons without any help. Hence, researchers designed these certain specific crystals with period poling structure, named as quasi-phase-matching (QPM). The QPM structure is designed with opposite poled direction which can periodically increase the conversion efficiency, and widen the frequency response range. Among these crystals, the one that is most widely used is the periodically poled lithium niobate (PPLN)[20].

Futherly, the wavelength and the bandwidth limitations inherent in natural phase matching has been broken caused by QPM which can be artificially controlled by the nonlinear polarization distribution within crystal. Harris proposed the PPLN crystal with the chirped QPM structure in SPDC[21]. In this millimeter-scale crystals, the nonlinear grating with linearly varying spatial frequencies, which help to achieve broadband phase. And the chirped QPM can further modulate with the linear or nonlinear polarization period along the propagation direction and it can make the wide frequency range satisfy the QPM condition at distinct positions in the nonlinear crystal[22, 21, 23]. It provides a novel approach for the generation of ultra broadband biphotons[24, 25, 26, 27, 28, 29]. Compared to type I SPDC[30, 31], the type II makes the signal and idler photons can be separated by birefringence. It can show more advantageous for the characterization and manipulation of quantum entanglement for the characteristic of influent frequency-non-degeneracy. Research indicates that the chirped QPM in type II SPDC can generate the ultra broadband biphotons with bandwidth of $300nm$[3] and the FWHM of the HOM interference can be compressed to $7.1fs$[24], which is helpful for the foundation of the single-cycle biphotons pulse.

Ref.[32] studied the single-cycle biphotons generated in chirp QPM PPKTP crystal, the joint spectral amplitude distributions are different between the PPKTP and PPLN crystals. Ref.[33] studied the biphotons generated through the nonlinear SPDC in chirp QPM PPLN crystal, suitable temperature angle may make the generated biphotons with wider frequency range. When considering

⋆ Corresponding author: linhb@tzvtc.edu.cn
⋆⋆ These authors contributed equally to this work

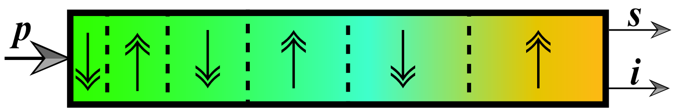

Figure 1. The Type II SPDC in the chirped QPM PPLN crystal

the temperature factor, Ref.[31] pay the attention on the noncollinear SPDC in type I, the suitable temperature is in the range of $0°C - 200°C$. The angle of the nonlinear is also should be suitable(about $\theta = 0.06$).

In this paper, we consider the biphotons generated through temperature dependent type II SPDC, to research how does the temperature influence the frequence response range, the Fedorov parameter, and the temporal width of the biphotons.

2. Theoretical Model

2.1. SPDC in a linearly chirped PPLN crystal

The monochromatic pump light with wavelength $\lambda_p = 0.42\mu m$ incidents into the chirp QPM PPLN crystal with its length $L = 2cm$[21]. As shown in fig 1, the interaction between the pump light and the crystal would make the pump light split into two photons simultaneously, named signal and idler with lower frequencies ω_s and ω_i, respectively. And their phase mismatching can be shown as following:

$$\Delta k(\omega, z) = k(\omega_p) - k(\omega) - k(\omega_p - \omega) - K(z), \tag{1}$$

Here, ω is the signal frequency and $\omega_p - \omega$ is the idler frequency for the reason of energy conservation that the sum of signal and idler frequency equals pump frequency: $\omega_p = \omega_s + \omega_i$. This law makes the biphotons generated in the nonlinear PPLN crystal show their entanglements. In this process, the wave number vector $k = n\omega/c$, where n is the refractive index for the PPLN crystal and c is the light speed in vacuum.

For the chirp QPM PPLN crystal, the poled grating periods Λ_n would be varying along the propagating direction, which can match the three photons wavelengths' phase mismatching. For simplicity, and to make more phase mismatching can be compensated, the poled grating periods can be designed with linearly chirped, which can be expressed as,

$$\Lambda_n(z) = \Lambda_0 + \xi z \tag{2}$$

where the ξ is viewed as the chirp rate for the poled grating periods, and Λ_0 is the first poled grating period for compensating the phase mismatching in the incident crystal. Then, the pump photon propagates along the axis of the nonlinear and split into two photons whose phases mismatched and can be compensated by the chirp poling period gratings and make the frequency response range (FRR) be wider. According to $K_0 = \frac{2\pi}{\Lambda_0}$, hence $K(z)$ in Eq.(3) can be expressed as:

$$K(z) = \frac{2\pi}{\Lambda(z)} = K_0 - \zeta z \tag{3}$$

Here, for simplicity, the chirped rate can be designed as linear(as shown in fig 1). And Eq.(3) can be rewrite as ζz, and ζ denotes the phase compensation chirped rate in the phase mismatching function. Compared with the poling grating periods chirp rate ξ, ζ plays a more significant and direct role in SPDC. Hence, let $K(z) = \zeta z$, and phase mismatching function $\Delta k(z)$ in Eq.(1) can be expressed as follows[21]:

$$\Delta k(\omega) = k(\omega_p) - k(\omega) - k(\omega_p - \omega) - K_0 \tag{4}$$

This equation shows the phase compensation relation between the intrinsic vector mismatching with the chirped QPM poled grating periods $K(z)$ [23].

The compensation for the phase mismatching function can make the more frequencies take part in parametric down-conversion process. Hence the adjust and control for the phase mismatching function is very important for SPDC. And there are many methods for adjust and control, including designing crystal structure, different frequency spectra, different kinds of crystals, etc.

2.2. Temperature dependence of Type II SPDC

According to thermal expansion and cold contraction, the lenghth of the nonlinear crystal would be affected by the varying of temperature. The lenghth of PPLN crystal can be expressed as[34]:

$$L(T) = L_0[1 + \alpha(T)(T - T_0)] \tag{5}$$

where L_0 is the crystal length with $T_0 = 25°C$, and $\alpha(T)$ is the thermal expansion coefficient. Compared with the whole crystal length, the poled grating periods $\Lambda_j(T)$ would also be influenced by the temperature according to Eq.(5). Hence, the sum of all the poled grating periods $\Sigma\Lambda_j(T)$ is equal to the whole PPLN crystal length $L(T)$. Based on the same expansion coefficient shown in Eq.(5), the temperature dependent chirp rate $\zeta(T)$ can be simply described as ζ without temperature.

To deeply understanding the temperature influence for the biphotons generated in type II SPDC, the refractive index function in wave number vector is associated with the temperature and can be expressed as follows[35, 36]:

$$n(\lambda, T) = \sqrt{A_1 + \frac{A_2 + B_1 R(T)}{\lambda^2 - [A_3 + B_2 R(T)]^2} + B_3 R(T) - A_4 \lambda^2}, \tag{6}$$

where λ is the wavelength of the light in microns. The temperature-dependent function $R(T) = (T - 24.5)(T + 570.5)$ [35]. And the unit of temperature T is degree Celsius. The values of $A_1, A_2, A_3, A_4, B_1, B_2$ and B_3 are the constants shown in Ref. [35]. Hence, the temperature dependent phase mismatching function can be expressed as:

$$\Delta k(\omega, z, T) = k(\omega_p, T) - k(\omega, T) - k(\omega_p - \omega, T) - K(z, T), \tag{7}$$

where $K(z,T) = \frac{2\pi}{\Lambda_0(T)} + \zeta(T)z$, and $\zeta(T)$ is temperature-dependent chirp rate. According to the thermal expansion and contraction of the nonlinear crystal, the length of crystal would be longer as the higher temperature. Meanwhile, the pole grating periods would be wider. They have the same thermal expansion coefficient, so the increase in their length is also the same as the temperature rises. It means that the chirp rate remains constant regardless of changes in temperature. And when $z = 0$, the initial phase mismatching function which stands for the left side of nonlinear can be defined as:

$$\Delta k_0(\omega, T) = \Delta k(\omega, z = 0, T) \tag{8}$$

2.3. Biphoton State in Chirp QPM PPLN

Under the regulation of the initial phase mismatching function, combined with SPDC in nonlinear crystals, the three wave mixed function of the biphotons can be expressed as:

$$|\Psi(T)\rangle = \int d\omega F(\omega, T) a^\dagger(\omega) a^\dagger(\omega_p - \omega)|0\rangle \tag{9}$$

Here, the unnormalized joint spectral amplitude function $F(\omega, T)$ can be expressed in terms of imaginary error functions $\mathrm{erfi}(x)$ [21]:

$$F(\omega, T) = \exp\left[\frac{-i\Delta k_0(\omega, T)^2}{2\zeta}\right] \times \left\{\mathrm{erfi}\left[\frac{(1+i)\Delta k_0(\omega, T)}{2\sqrt{\zeta}}\right] - \mathrm{erfi}\left[\frac{(1+i)[\Delta k_0(\omega, T) + \zeta L(T)]}{2\sqrt{\zeta}}\right]\right\} \tag{10}$$

The joint spectral amplitude function of the biphotons generated in the chirped QPM including the quadratic phase factor. And the ultra broadband spectrum pulse cannot be effectively compressed into an ultrashort pulse for this quadratic phase. Hence, for the effectively compression of the pulse, the quadratic phase factor of the joint spectral amplitude function can be compensated according to the method in Ref.[21], and the compensation function can be shown as:

$$F_C(\omega, T) = \exp\left\{i\frac{\Delta k_0(\omega, T)^2}{2\zeta} - i\left[k(\omega, T) + k(\omega_p - \omega, T)\right] L(T)\right\}, \tag{11}$$

Then, the generated signal and idler photons, can propagate the dispersive and delay medium, respectively. They can simultaneously arrive at the ultrafast

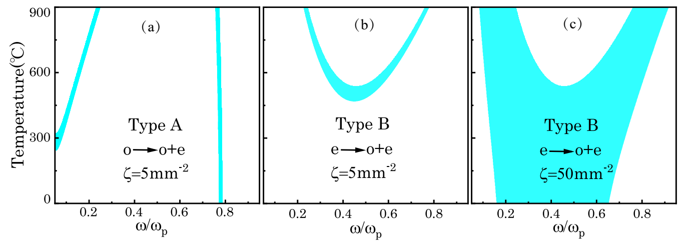

Figure 2. The initial phase mismatch function Δk_0 within the range of $-\zeta L \leq \Delta k_0 \leq 0$ versus the frequency and temperature of type A ($o \to o + e$) with (a). $\zeta = 5\mathrm{mm}^{-2}$; and type B ($e \to o + e$) with (b). $\zeta = 0.5\mathrm{mm}^{-2}$; (c). $\zeta = 50\mathrm{mm}^{-2}$

correlator[37], and generate the sum frequency photon with frequency ω_{sum} which is equal with the frequency of pump photon. And the ultrashort pulse with single cycle can also be detected by homodyne detection between the two photons[21].

3. Analysis and Discussion

As discussed in above, fig 2 shows the relationship between the frequency response range of initial phase matching function $\Delta k_0(\omega, z = 0, T)$ and temperature T in type II SPDC. To achieve the phase compensation effect, Δk should be in the range of $-\zeta L \leq \Delta k \leq 0$.

In this paper, for the type II SPDC, we define $o \to o+e$ and $e \to o + e$ as type A and type B, respectively. Here, o and e represent the polarization of ordinary and extraordinary lights, respectively. The initial phase mismatching function Δk_0 versus frequency and temperature can be shown as fig 2. In this figure, it can be observed that the structures of phase mismatching function for type A and type B are asymmetric about $\omega = \omega_p/2$. It is essential different with type 0 and type I SPDC. The reason is that they are different types for SPDC. The photons can be changed from one polarization state to another, and the generated photons are different polarizations. Hence, their phase mismatching functions are asymmetric about $\omega = \omega_p/2$.

By comparison, for type A, the temperature influence is weak for the FRR in the range of $\omega > \omega_p/2$. The main influence for the part is the chirp rate ζ. The higher chirp rate, the wider FRR. However, in the range of $\omega < \omega_p/2$, there would no frequency response range until the temperature $T > 250°C$. And the roughness would be thicker as the chirp rate ζ be higher. There is no any frequency response range near $\omega = \omega_p/2$, which is essential different with type B. In type B, the frequency range is mainly around $\omega = \omega_p/2$. And for the small chirp rate $\zeta = 5mm^{-2}$, the frequency response range would emerge only within the temperature $T > 450°C$. And the structure of frequency response range is an asymmetric parabolic-like shape. The higher chirp rate would make the structure of frequency range be wilder, like the trunk of a big tree.(see fig 2 (c)).

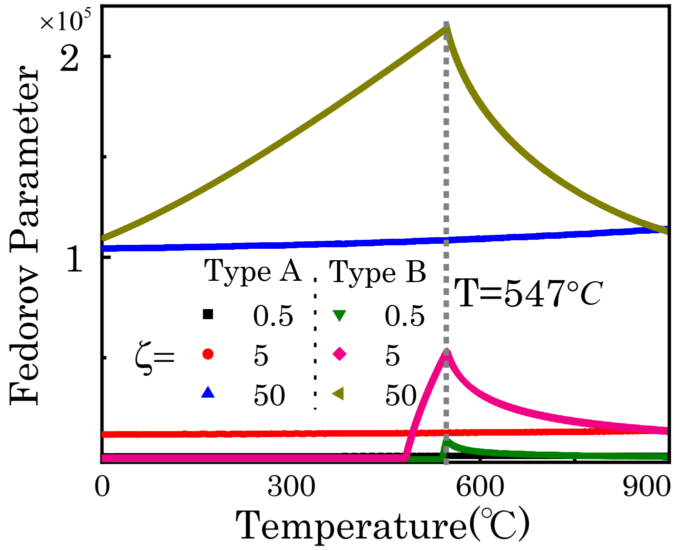

Figure 3. The Fedorov parameter(FP) in type A and type B versus the temperature

Hence, the larger chirp would essentially widen the frequency response range of phase mismatching function both of type A and type B. It is similar to the situation of type 0 and type I SPDC. The higher chirp rate would effectively widen FRR in type 0 ($o \to o + o$ and $e \to e + e$) and type I ($o \to e + e$ and $e \to o + o$). The relationship of three waves' polarizations determine many characteristics, such as FRR, symmetry characteristics. The higher symmetry and the larger chirp rate ζ, the wider FRR. However, the temperature of nonlinear PPLN crystal plays weaker role for biphotons generated in SPDC.

The entanglement of biphotons is determined by the frequency response range of the phase mismatching function, the nonlinear crystal temperature and the crystal type. And the Fedorov Parameter (FP), which represents the entanglement degree, is determined by frequency response width and the pump light's bandwidth[21]. Hence, the larger chirp rate ζ can effectively rise the FP value, such as shown in fig 3. When $\zeta = 50mm^{-2}$, the FP value are larger then 10^5. However, the FP value much less when $\zeta = 0.5mm^{-2}$ or $5mm^{-2}$. It can be observed that the temperature's influence is very weak for type A, the line is almost horizontal. However, the temperature's influence is obvious for type B. The FP would reach the highest value within the same temperature for different chirp rates. These points match with the lowest point of listric surfaces in fig 2(b) and (c). The frequency response range would extend towards the lower temperature in different chirp rates, not higher temperature. Hence the lowest points of FRR within the same temperature. When $\zeta = 0.5mm^{-2}$, the temperature would not influence the FP until $T > 450°C$ in type B. Then, the FP value would be larger and larger as the temperature be higher. Until $T = 547°C$, the FP value would be highest. After that, the temperature becomes higher, the FP value would be smaller. This matches with the features shown in fig 2(b), the two mutually confirm each other. When $\zeta = 50mm^{-2}$, the FP value of type B would increase linearly with the rise in temperature, and would reach the highest with $T = 547°C$. Then the FP value would decrease rapidly as the temperature rises. This matches with the feature shown in fig 2(c).

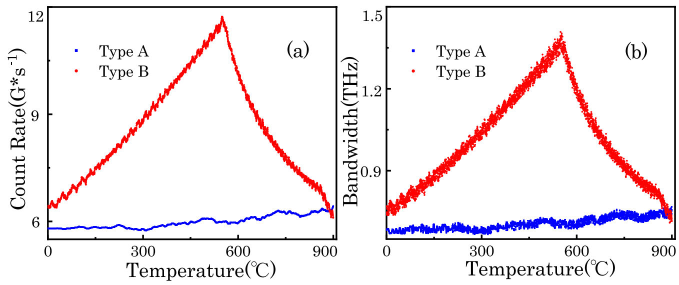

Figure 4. (a) The count rate and (b) the bandwidth for the biphotons versus the temperature of type A and type B in the chirp QPM PPLN during type II SPDC.

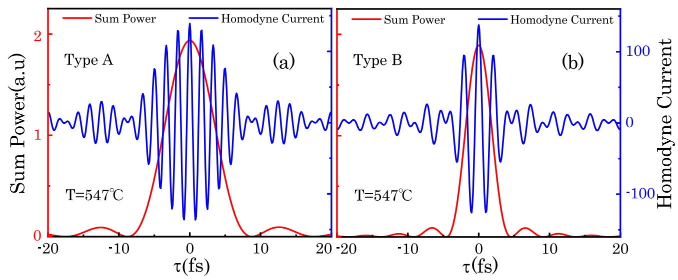

Figure 5. The sum power and homodyne current of the biphotons detected by homodyning with the temperature $T = 547°C$ of type A and type B during type II SPDC.

As the discussion shown above, the FRR of type A and type B SPDC and the FP value are mainly determined by the factor of the chirp rate for the QPM. The FP value is small within small chirp rate ζ. Hence, we discuss the case of $\zeta = 50mm^{-2}$, the FRR of Δk_0 can be shown in fig 2(c) and the FP versus temperature shown in fig 3. The count rate and the bandwidth of entangled biphotons generated through SPDC influenced by the temperature is shown in fig 4. In this figure, the temperature's influence is very weak for count rate and bandwidth of biphotons in type A.

However, in type B, the higher temperature can effectively rise the count rate and the bandwidth of the entanglement biphotons. They wouldn't be the highest until the temperature $T = 547°C$. Then, with the higher temperature, the count rate and bandwidth of biphotons would decrease. This matches with the FP versus temperature in type B within chirp rate $\zeta = 50mm^{-2}$ shown in fig 3. And also in the fig 2(c).

With the help of the method proposed in Ref.[21], the entangled signal and idler photons generated through SPDC would propagate dispersive and delay medium, respectively, and can arrival at the ultrafast correlator simultaneously[37]. They can generate a new photon with their sum frequency (ω_{sum}), which is the same with pump photon frequency ω_p. Hence, for both of them, they can be detected by the homodyne detection and can generate the ultrashort biphotons with single cycle. When chirp rate $\zeta = 50mm^{-2}$, temperature $T = 547°C$, the type II SPDC in the chirped QPM PPLN crystal, the sum power and homodyne current of biphotons in type A and type B can be shown in fig 5. By comparison, the temporal width of the ultrashort biphotons generated in both types can be shorter than $10fs$. Especially in type B, the temporal width of the ultrashort biphotons reaches $5fs$, with the single cycle level as predicted in Ref.[21]

4. Conclusion

We investigated the temperature dependent process of type II SPDC, which can generate the single cycle biphotons in the chirp QPM PPLN crystal. For both of type II SPDC ($o \rightarrow o + e$ and $e \rightarrow o + e$), the characteristics of biphotons would be influenced by many factors, such as the chirp rates and the temperature of the crystal. The appropriate temperature would make the frequency response range be wider and the FP be higher, and the generated biphotons can reach the single cycle level.

Acknowledgments

W. J. sincerely thanks S. E. Harris for his mathematica codes.

Funding

This research was funded by the Taizhou High-Level Talent Special Support Program Project (Tai Talent Ling [2020] No.4) and Taizhou Vocational & Technical College's Key Research Project for 2026 (2026ZD05).

Conflicts of interest

The authors have nothing to disclose.

Data availability statement

This article has no associated data generated or analyzed data associated with this article cannot be disclosed due to ethical reason.

Author contribution statement

Writing-Original Draft Preparation, Review & Editing, H. L.; Supervision, J.W.

Ethical approval

This is Ethical Approval text here.

Informed consent

This is Informed Consent text here.

Glossary

This is Glossary text here.

Supplementary material

This is Supplementary Material text here.

References

1. You D, Jones RR, Bucksbaum PH, Dykaar DR, Generation of high-power sub-single-cycle 500-fs electromagnetic pulses, Opt. Lett ,4, 290 (1993). https://opg.optica.org/ol/abstract.cfm?URI=ol-18-4-290
2. Brabec T, Krausz F, Intense few-cycle laser fields: Frontiers of nonlinear optics, Rev. Mod. Phys.,72, 545 (2000). https://link.aps.org/doi/10.1103/RevModPhys.72.545
3. Shverdin MY, Walker DR, Yavuz DD, Yin GY, Harris SE, Generation of a Single-Cycle Optical Pulse, Phys. Rev. Lett., 94, 033904 (2005). https://link.aps.org/doi/10.1103/PhysRevLett.94.033904
4. Sansone G, et al, Isolated Single-Cycle Attosecond Pulses, Science, 314, 5789 (2006). https://www.science.org/doi/abs/10.1126/science.1132838
5. Corkum P, Krausz F, Attosecond science, Nature physics, 3, 381 (2007). https://doi.org/10.1038/nphys620
6. Chen WJ, et al, Sub-Single-Cycle Optical Pulse Train with Constant Carrier Envelope Phase, Phys. Rev. Lett.,16, 163906 (2008). https://link.aps.org/doi/10.1103/PhysRevLett.100.163906
7. Kitaeva GK, Kornienko V V, Leontyev AA, Shepelev AV, Generation of optical signal and terahertz idler photons by spontaneous parametric down-conversion, Phys. Rev. A, 98, 063844 (2018). https://link.aps.org/doi/10.1103/PhysRevA.98.063844
8. Haase B, et al, Spontaneous parametric down-conversion of photons at 660 nm to the terahertz and sub-terahertz frequency range, Opt. Express, 27, 7458 (2019). https://opg.optica.org/oe/abstract.cfm?URI=oe-27-5-7458
9. Marceau C, Gingras G, Witzel B, Excitation with Effective Subcycle Laser Pulses, Phys. Rev. Lett.,20, 203005 (2013). https://link.aps.org/doi/10.1103/PhysRevLett.111.203005
10. Wang ZY, Lin Q, Wang ZY, Single-cycle electromagnetic pulses produced by oscillating electric dipoles, Phys. Rev. E., 67, 016503 (2003). 10.1103/PhysRevE.67.016503
11. Lin Q, Zheng J, Wilhelm B, Subcycle Pulsed Focused Vector Beams, Phys. Rev. Lett., 97, 253902(2006). https://link.aps.org/doi/10.1103/PhysRevLett.97.253902
12. Fraine A, Minaeva O, Simon DS, Egorov R, Sergienko AV, Broadband source of polarization entangled photons, Opt. Lett.,37, 1910(2012). https://opg.optica.org/ol/abstract.cfm?URI=ol-37-11-1910
13. Chuu CS, Harris SE, Ultrabright backward-wave biphoton source, Phys. Rev. A, 83, 061803(R) (2011). https://link.aps.org/doi/10.1103/PhysRevA.83.061803
14. Dai HN, et al, Holographic Storage of Biphoton Entanglement, Phys. Rev. Lett., 108, 210501(2012). 10.1103/PhysRevLett.108.210501

15. Katamadze KG, Borshchevskaya NA, Dyakonov IV, Paterova A V, Kulik SP, Broadband biphotons in a single spatial mode, Phys. Rev. A, 92, 023812 (2015). https://link.aps.org/doi/10.1103/PhysRevA.92.023812
16. Fedorov MV, Efremov MA, Kazakov AE, Chan KW, Law CK, Eberly JH, Packet narrowing and quantum entanglement in photoionization and photodissociation, Phys. Rev. A, 69, 052117(2004). https://link.aps.org/doi/10.1103/PhysRevA.69.052117
17. Fedorov MV, Efremov MA, Volkov PA, Moreva EV, Straupe SS, Kulik SP, Anisotropically and High Entanglement of Biphoton States Generated in Spontaneous Parametric Down-Conversion, Phys. Rev. Lett., 99, 063901 (2007). https://link.aps.org/doi/10.1103/PhysRevLett.99.063901
18. Tanaka A, et al, Noncollinear parametric fluorescence by chirped quasi-phase matching for monocycle temporal entanglement, Opt. Express, 20, 25228 (2012). https://opg.optica.org/oe/abstract.cfm?URI=oe-20-23-25228
19. Kuznetsov KA, et al., Nonlinear interference in the strongly nondegenerate regime and Schmidt mode analysis, Phys. Rev. A, 101, 053843(2020). https://link.aps.org/doi/10.1103/PhysRevA.101.053843
20. Myers LE, et al., Quasi-phase-matched optical parametric oscillators in bulk periodically poled LiNbO3 , J. Opt. Soc. Am. B, 12, 2102 (1995). https://opg.optica.org/josab/abstract.cfm?URI=josab-12-11-2102
21. Harris SE, Chirp and Compress: Toward Single-Cycle Biphotons, Phys. Rev. Lett., 98, 063602 (2007). https://link.aps.org/doi/10.1103/PhysRevLett.98.063602
22. Arbore MA, Marco O, Fejer MM, Pulse compression during second-harmonic generation in aperiodic quasi-phase-matching gratings, Opt. Lett., 22, 865 (1997). https://opg.optica.org/ol/abstract.cfm?URI=ol-22-12-865
23. Mathieu CL, Afeyan B, Fejer MM, Optical parametric amplifiers using chirped quasi-phase-matching gratings I: practical design formulas, J. Opt. Soc. Am. B, 25, 463 (2008). https://opg.optica.org/josab/abstract.cfm?URI=josab-25-4-463
24. Nasr MB, et al., Ultrabroadband Biphotons Generated via Chirped Quasi-Phase-Matched Optical Parametric Down-Conversion, Phys. Rev. Lett., 100, 183601 (2008). https://link.aps.org/doi/10.1103/PhysRevLett.100.183601
25. Brida G, et al., Biphoton compression in a standard optical fiber: Exact numerical calculation, Phys. Rev. A, 81, 053828 (2010). https://link.aps.org/doi/10.1103/PhysRevA.81.053828
26. Sensarn S, Yin GY, Harris SE, Generation and Compression of Chirped Biphotons, Phys. Rev. Lett., 104, 253602(2010). https://link.aps.org/doi/10.1103/PhysRevLett.104.253602
27. Horoshko DB, Kolobov MI, Towards single-cycle squeezing in chirped quasi-phase-matched optical parametric down-conversion, Phys. Rev. A, 88, 033806(2013). https://link.aps.org/doi/10.1103/PhysRevA.88.033806
28. Li BH, et al, Temporal compression and shaping of chirped biphotons using Fresnel-inspired binary phase shaping, Phys. Rev. A, 91, 023827 (2015). https://link.aps.org/doi/10.1103/PhysRevA.91.023827
29. Horoshko DB, Kolobov MI, Generation of monocycle squeezed light in chirped quasi-phase-matched nonlinear crystals, Phys. Rev. A, 95, 033837(2017). https://link.aps.org/doi/10.1103/PhysRevA.95.033837
30. Laudenbach F, et al., Modelling parametric down-conversion yielding spectrally pure photon pairs, Opt. Express, 24, 2712(2016). https://opg.optica.org/oe/abstract.cfm?URI=oe-24-3-2712
31. Lin HB, Wang JB, The temperature-dependent in non-collinear SPDC for generating biphotons with single cycles, J. Eur. Opt. Society-Rapid Publ., 21, 38, (2025), https://doi.org/10.1051/jeos/2025033
32. JB Wang, HB Lin, The single-cycle biphotons generated by SPDC in chirped QPM PPKTP crystal, Journal of Nonlinear Optical Physics & Materials, 34, 05, (2025), https://doi.org/10.1142/S0218863524500061
33. JB Wang, HB Lin, The single-cycle biphotons generated by noncollinear SPDC in the chirped QPM crystals, J. Eur. Opt. Society-Rapid Publ., 20, 1, (2024), https://doi.org/10.1051/jeos/2024004
34. Pignatiello F, et al., Measurement of the thermal expansion coefficients of ferroelectric crystals by a moiré interferometer.Opt. Comm. 277, 1 (2007), https://doi.org/10.1016/j.optcom.2007.04.045.
35. Edwards GJ, Lawrence M, A temperature-dependent dispersion equation for congruently grown lithium niobate, Optical and Quantum Electronics, 16, 373(1984). https://doi.org/10.1007/BF00620081
36. Pignatiello F, et al., Measurement of the thermal expansion coefficients of ferroelectric crystals by a moiré interferometer, Optics Communications, 277, 14(2007). https://www.sciencedirect.com/science/article/pii/S0030401807004506
37. Pe'er A, et al, Temporal Shaping of Entangled Photons, Phys. Rev. Lett., 94, 073601 (2005). https://link.aps.org/doi/10.1103/PhysRevLett.94.073601

Appendix

This is Appendix text here.